AJNR

A Simplified Arteriovenous Malformation Model in Sheep: Feasibility Study

Zhong Qian, Salvador Climent, Manuel Maynar, Jesus Usón-Garallo, Marco A. Lima-Rodrigues, Camen Calles, Hugh Robertson and Wilfrido R. Castañeda-Zúñiga

AJNR Am J Neuroradiol 1999, 20 (5) 765-770
http://www.ajnr.org/content/20/5/765

AJNR Am J Neuroradiol 20:765–770, May 1999

A Simplified Arteriovenous Malformation Model in Sheep: Feasibility Study

Zhong Qian, Salvador Climent, Manuel Maynar, Jesus Usón-Garallo, Marco A. Lima-Rodrigues, Camen Calles, Hugh Robertson, and Wilfrido R. Castañeda-Zúñiga

BACKGROUND AND PURPOSE: **Recently, a swine model of a cerebral arteriovenous malformation (AVM) has been developed that closely resembles a human AVM of the brain. The creation of such a model requires sophisticated neurointerventional techniques. The purpose of this study was to develop a simple and cost-effective AVM animal model that does not require additional endovascular techniques.**

METHODS: **A surgical anastomosis was created in seven sheep between the common carotid artery and the ipsilateral jugular vein, followed by ligation of the jugular vein above the anastomosis and of the proximal common carotid artery below the anastomosis. The anastomosis was created on the left side in four animals and on the right side in three. Cerebral angiography from the contralateral carotid artery was performed before and immediately after surgery to delineate the relevant cerebral vascular anatomy and to determine the direction of blood flow.**

RESULTS: **An angiographic appearance simulating an AVM was found in all the animals. The ramus anastomoticus and arteria anastomotica functioned as the feeding vessels to the rete mirabile, which represented the nidus in our model, and to the jugular vein, which represented the draining vein from the malformation. Extensive collateral flow through the rete mirabile into the distal segment of the external carotid artery above the ligature was observed angiographically, with retrograde flow through the surgical anastomosis into the jugular vein.**

CONCLUSION: **A simple surgically created experimental model for cerebral AVMs was developed in sheep without the need for additional complex endovascular catheter manipulations of intracranial branches. Such an animal model can substantially reduce the cost of research and training in the neurointerventional or radiosurgical management of AVMs.**

Cerebral arteriovenous malformations (AVMs) have the potential for causing intracranial hemorrhage, progressive neurologic deficit, and death. The traditional treatment is surgical excision of the lesion; however, depending on location and size, surgical intervention is not always possible and can be associated with severe complications (1–4). Recent advances in catheter technology, imaging techniques, and sophisticated radiation therapy have enhanced the role of endovascular catheter therapy and radiosurgery in the management of cerebral AVMs. Despite encouraging experimental and clinical results, many unsolved problems remain, especially in regard to the behavior of AVMs after treatment. This is due in part to the lack of an in vivo AVM model that can be used to elucidate the posttreatment pathologic and hemodynamic changes. Recently, an animal model in swine resembling a human AVM was reported by Massoud et al (5), who created the AVM model by diverting and increasing blood flow through the retia mirabilia. This was achieved by the surgical creation of a side-to-side anastomosis between the carotid artery and jugular vein, together with the endovascular embolization of several ipsilateral carotid artery branches. This method constituted a breakthrough in research on cerebral AVMs. Nonetheless, establishment of this model requires highly sophisticated neurointerventional skills and expensive microcatheters, wires, and detachable balloons.

Some of the tributaries of the carotid arteries that require occlusion in the swine model do not exist in sheep. We therefore speculated that the retia mirabilia in sheep could be shown after a simple ca-

Received August 21, 1998; accepted after revision January 27, 1999.

Presented at the annual meeting of the American Society of Neuroradiology, Philadelphia, May 1998.

From the Department of Radiology, LSU Medical Center at New Orleans (Z.Q., H.R., W.R.C-Z.); the Department of Anatomy, University of Zaragoza, Spain (S.C.); Las Palmas de Gran Canaria University, Spain (M.M.); and the Minimally Invasive Surgery Center, Cáceres, Spain (M.M., J.U-G., M.A.L-R., C.C.).

Address reprint requests to Zhong Qian, MD, Department of Radiology, LSU Medical Center, 1542 Tulane Ave, New Orleans, LA, 70112.

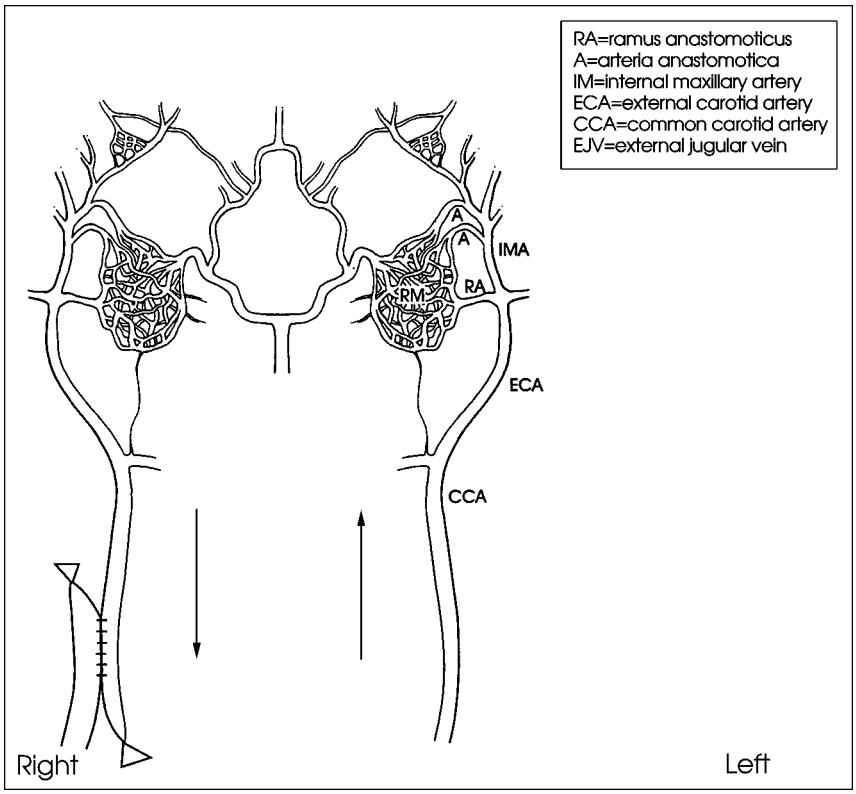

FIG 1. Schematic representation of an AVM model in sheep. Circulatory flow is diverted from the contralateral side (*left*) of the carotid artery through both carotid retia (RM) to the right carotid artery and jugular vein with retrograde flow following surgical creation of an anastomosis. Note the blood flow direction (*arrows*) after creation of a carotid-jugular anastomosis.

rotid-jugular surgical anastomosis. If this premise was correct, creation of the AVM animal model would be more practical and cost-effective. The purpose of our study was to evaluate the feasibility of creating an in vivo AVM model in sheep without the need for additional sophisticated neurointerventional procedures.

Methods

The study was carried out in compliance with the Guide for the Care and Use of Laboratory Animals (National Research Council, 1996). The sheep were transported to our animal care facilities and quarantined for 1 week before the procedure. One day before the operation, each animal was fasted overnight. Preanesthetic medication included the intravenous injection of atropine (1 mg) for minimizing salivary secretion and propofol (2 mg/kg) for sedation. After intubation, seven Merino sheep (three male, four female) ranging in weight from 62 to 80 kg were given 2% halothane for general anesthesia. Vital signs were closely watched. Anesthesia and respiratory depth were controlled by monitoring heart rate, blood pressure, cardiac output, body temperature, end tidal CO_2, and blood O_2 saturation via a computerized anesthetic machine (Ohmeda Excel 210 SE, Madrid, Spain).

Preprocedural Angiography

The right groin was prepared for percutaneous femoral arterial access. The superficial femoral artery was punctured using the Seldinger technique, and a 6F introducer sheath was inserted over a guidewire. Because the brachiocephalic vessels in sheep arise via a single trunk from the ascending aorta, a 5F Simmons-Sidewinder catheter (AngioDynamics, Glens Falls, NY) was used to catheterize the carotid artery. As soon as the catheter tip was placed in the carotid artery, a guidewire was passed and the Simmons catheter was exchanged for a 5F straight catheter with multiple side holes (Royal Flush II, Cook, Bloomington, IN). Selective carotid arteriography was performed through the straight catheter using 10 mL of 60% Urografin (Schering, Germany) injected at a rate of 5 mL/s to delineate the normal cerebral vascular anatomy in both anteroposterior and lateral views. Right and left anterior oblique (tilted 30°) views were also obtained.

Surgical Creation of the Anastomosis

Under surgical sterile conditions, a 10-cm-long incision was made in the neck on the right side in four sheep and on the left side in three. Five-centimeter-long segments of the common carotid artery (CCA) and the external jugular vein (EJV) were exposed and isolated. After the perivascular connecting tissues were carefully removed, each end of the isolated vessels was clamped with a vascular miniclamp to temporarily block blood flow through the segment during surgical creation of the anastomosis. A 2-cm longitudinal straight incision was made in both the CCA and the EJV. The residual intraluminal blood was washed out with Ringer's solution. The side-to-side anastomosis between the CCA and EJV was created using a continuous 7–0 prolene suture. The clamps were then released from the vessels. In order to divert the blood flow from the CCA to the ipsilateral EJV, the CCA was ligated 1 cm below the anastomosis (Fig 1). The incision was then sutured in layers.

Postprocedural Angiography

Postprocedural cerebral angiography was performed from the contralateral side immediately after surgery to delineate the postsurgical cerebral vascular anatomy and to evaluate the concomitant hemodynamic changes. The position of the animal and location of the catheter tip were the same as for preprocedural angiography. Using a BV-300 (Phillips, Best, the Netherlands), a mobile digital angiographic system, we acquired digital subtraction angiograms at a speed of 12 frames per second.

FIG 2. Normal cerebrovascular anatomy on left common carotid arteriogram before surgery.

A, Lateral view shows the rete mirabile (*arrowheads*) supplied by the ramus anastomoticus (*short arrow*) and the arteria anastomotica (*long arrow*).

B, Anteroposterior view shows unilateral rete mirabile (*arrowheads*) along with its feeding vessels, including the ramus anastomoticus (*short arrow*), the arteria anastomotica (*long arrow*), and the IMA (*open arrows*).

Preparation of a Corrosion Cast of the Retia Mirabilia and Associated Arteries

To understand the anatomic structures of the retia mirabilia and associated vascular supply better, a corrosion cast was made in two healthy sheep. The detailed technique for the creation of a corrosion cast of a vascular structure has been well described (6). We slightly modified that technique based on the availability of chemical supplies. Briefly, an incision is made on the neck on both sides. After the animals are heparinized and sacrificed by injection of 2% KCl (20 mL), the CCAs on both sides are isolated and cannulated with a 10F guiding catheter. The CCAs are then purged with 2 to 3 L of normal saline by hand injection. As soon as flushing is completed, 30 mL of 5% buffered formalin is quickly injected into the CCAs, followed by introduction of the specially prepared mixed solution containing 80 mL of epoxy resin Araldit CY223 (Ciba Geigy, Madrid, Spain), 28 mL of polyamine HY2967 (Ciba Geigy), and 2 mL of red ink DW0133 (Ciba Geigy). Vascular filling was established by observing the uniform change in color of the tongue. The polymerization process took 16 to 20 hours to complete, while the animal was kept in a cooler at a temperature of 4°C. Twenty hours after injection of the polymer solution, the animal was brought back to our laboratory and its head was severed at the level of the third or fourth cervical vertebral body. Following removal of the skin, the head was soaked in 20% NaOH solution. The solution was refreshed every 48 hours. Every 24 hours, the head was lifted and pressure-washed by tap water in order to accelerate the corrosion process, in which perivascular tissues were removed. The corroded vascular cast was placed in concentrated HCl for 5 minutes and was then carefully cleaned by rinsing in distilled water.

Results

Angiographic evaluation and surgical creation of the anastomosis were successfully accomplished in all animals. There was no technical failure and no associated mortality. The main purpose of this study was to prove the hypothesis that the retia mirabilia and the diversion of blood can be demonstrated in sheep after surgical anastomosis. Because endoluminal or radiosurgical therapies were not attempted, all the experimental animals were sacrificed after the AVM model was established.

Preprocedural selective common carotid angiograms confirmed the existence of normal cerebral vascular anatomy. The unilateral rete mirabile was readily identified as an oval-shaped arterial plexus in the early angiographic phase, approximately 12 mm in width and 20 mm in length (Fig 2). Blood flow to the rete mirabile was supplied mainly by the arteria anastomotica anteriorly and by the ramus anastomoticus posteriorly, both branches of the internal maxillary artery (IMA). The IMA represents the continuation of the external carotid artery (ECA), which itself is an extension of the CCA after giving off the occipital artery. In the sheep, the internal carotid artery is absent proximal to the rete. The abundant retia mirabilia vessels anteromedially reconstitute the internal carotid arteries, which then join the circle of Willis (Fig 3). It was noted that the retia mirabilia on the anastomotic side was not opacified during preprocedural carotid angiography (Fig 2B).

Surgical creation of the anastomosis was easily carried out. After brief training by a vascular surgeon, nonsurgeons were able to perform the procedure without difficulty. After the anastomosis was created and the vascular clamps removed, a significant dilatation of the EJV was observed with a strong pulse. Turbulence could be palpated on the jugular vein, indicating rapid flow through the shunt from the carotid artery to the jugular vein. During and after surgery, there were no significant changes in vital signs or systemic blood pressure.

Postprocedural cerebral angiography from the contralateral carotid artery demonstrated extensive collateral flow across the retia mirabilia to the IMA, ECA, and CCA cephalad to the ligation. Most of this blood flow went in a retrograde direction toward the EJV across the surgical anastomosis. There was insignificant orthograde flow in the distal IMA beyond the orifice of the arteria anastomotica on the anastomotic side. No occipital artery on the surgical side was identified on the angiogram. These manifestations indicate that the vast majority of blood flow from the retia mirabilia was diverted into the jugular vein through the anastomosis. The retia mirabilia on both sides were distinctly delineated in the early and middle phases of the angiograms. An angiographic appearance simulating an AVM nidus was demonstrated in all animals (Fig 4).

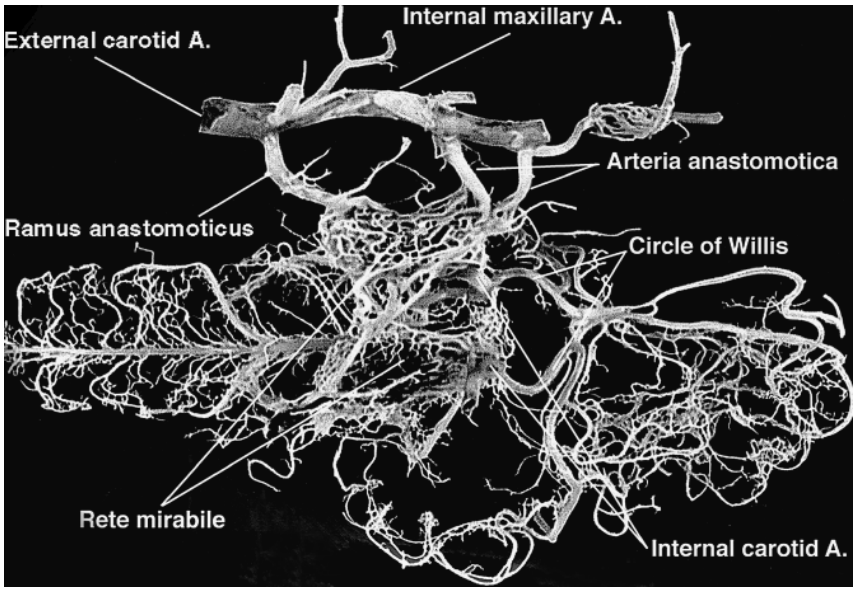

FIG 3. Photograph of the corrosion cast of the cerebrovascular anatomy on ventral view in the sheep shows the rete mirabile and its associated arteries compared with angiograms. Note that the internal carotid artery, a single large arterial trunk, bends sharply to join the circle of Willis.

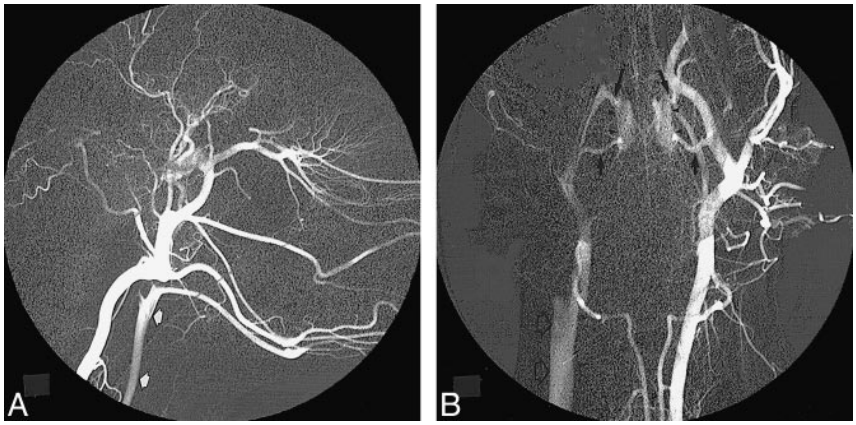

FIG 4. Left common carotid angiogram immediately after surgical creation of the anastomosis.

A, The carotid artery (*arrows*) on the anastomotic side is opacified in the early phase, indicating a high-flow diversion from catheterized side.

B, Bilateral retia mirabilia (*arrowheads*) are clearly identified, simulating an AVM nidus. The ramus anastomoticus (*short arrows*) and arteria anastomotica (*long arrows*), supplying the rete structure, represent the feeding vessels, while the same vessels on the anastomotic side act as the draining veins, emptying into the right jugular vein (*open arrows*) through the anastomosis.

Discussion

The use of the rete mirabile as a model of an AVM nidus has been described by several authors for endoluminal and radiosurgical therapies (5, 7–9). In many mammals, especially in the artiodactyl, blood supply to the brain comes from the carotid rete, which consists of a well-developed compact vascular network surrounded by the cavernous sinus at the base of the brain. The exact location of the rete in relationship to the base of the skull varies with animal species. In the sheep, pig, goat, and ox, the rete lies within the skull, whereas in the cat, the rete is located extracranially. The pig rete is situated more posteriorly than in other artiodactyls. There is no carotid rete structure in the dog, rabbit, and rat (10). The precise functions of the carotid rete remain unclear, despite some speculation on its function in heat exchange (11), oxygen exchange (12), regulation of blood flow to the brain (9), and diving ability in cetaceans (13).

The configuration of the carotid rete structure is similar to that of an AVM nidus in many aspects. The fine network of microarteries of the rete appears to be akin to the plexiform nidus of an AVM; the diameter of the individual rete vessels, ranging from 120 to 350 μm, is comparable to that of the cerebral AVM nidus, which averages 265 μm (5, 10, 14). Additionally, the rete was found to have the same biological response to glue embolization injury as do cerebral AVMs (15). Therefore, it is an ideal natural structure for use as an in vivo model for research and training in innovative therapies for cerebral AVMs. It has been noted that in a normal animal, the rete mirabile does not possess a high-flow hemodynamic pattern such as that observed in human cerebral AVMs, because it virtually represents an arterio-arterial shunt with a minimum pressure gradient, whereas AVMs are arteriovenous shunts with a large pressure gradient. This dilemma has been successfully resolved by the creation of a unilateral arteriovenous fistula by anastomosis between the carotid artery and the jugular vein (5). By using this surgical technique, the jugular vein draws abundant blood flow through the anastomosis from the ipsilateral carotid artery, and the mean pressure gradient across the bilateral retia can increase to approximately 21 mm Hg (16). Ligation of the carotid artery caudad to the anasto-

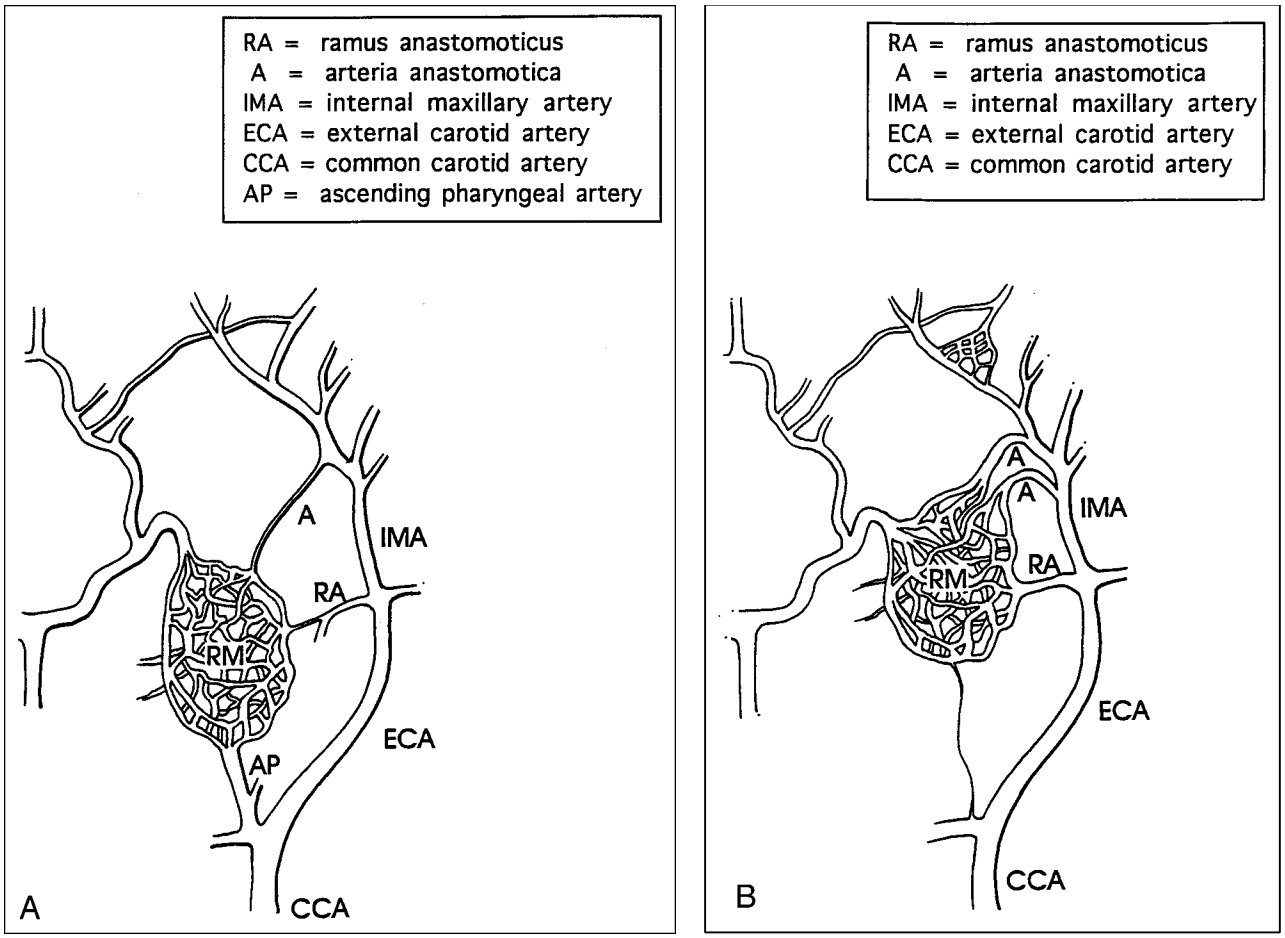

FIG 5. Schematic drawings show comparison of the rete mirabilia and the supply arteries in the pig and sheep.

A, In the pig, the rete mirabile receives most of its blood supply from the ascending pharyngeal artery, whereas only a small amount of flow is derived from branches of the IMA.

B, In the sheep, the fetal ascending pharyngeal artery undergoes atrophy, becoming a residual thread after birth. Branches of the IMA, the ramus anastomoticus, and the arteria anastomotica form the major arterial contributions to the rete mirabile.

mosis, blocking orthograde flow, also contributes to the increased pressure gradient. A diverted high-flow is, therefore, produced across the nidus, which resembles a cerebral AVM in humans.

Recently, Massoud et al (5) reported a successful AVM model in swine with the surgical creation of carotid-jugular fistula, followed by the endovascular occlusion of several tributaries of the carotid artery, including the ascending pharyngeal artery, the occipital artery, and the ECA on the anastomotic side. This elegant work demonstrated the technical feasibility of creating an in vivo model resembling cerebral AVMs in humans. In the pig, the carotid rete mirabile receives most of its blood supply from the ascending pharyngeal artery, whereas only a very small amount of flow is derived from branches of the IMA (Fig 5A). In this model, in order to maximize the postoperative diversion of blood flow into the EJV, it is necessary to embolize the occipital artery and the muscular branch of the ascending pharyngeal artery on the anastomotic side. Otherwise, the direct route from the rete to the anastomosis will be hampered by the participation of other arteries as major collateral pathways (5). In the sheep model, however, the arteries supplying the rete mirabile differ from those in the pig. In the sheep, a well-formed ascending pharyngeal artery is found in the fetus, which subsequently undergoes atrophy, ending as a residual thread after birth (Fig 5B). Major sources of blood supply to the carotid rete include a single ramus anastomoticus and two or three anastomotic arteries (the branches of the IMA) on each side.

We assumed that the pattern of circulatory diversion across the retia would be adequate without the need for perioperative endovascular arterial branch occlusion, because of the difference in vascular anatomy and the absence of the pharyngeal artery in sheep. The results of this experiment proved our assumption to be correct. Nonetheless, the mechanisms contributing to the improvement in rete blood flow are not yet fully understood, and other factors may contribute to this phenomenon. After giving off the ramus anastomoticus and the arteria anastomotica, the diameter of the IMA in sheep becomes smaller, unlike pigs in which the ECA maintains almost the same vessel diameter after giving off the ascending pharyngeal artery that

supplies the carotid rete. This may explain why after surgery, the diverted blood flow readily empties to the jugular vein in sheep without the need to occlude other arterial branches. In addition, the flow autoregulatory mechanism of the interretial network may be more sensitive to pressure gradient changes in the sheep than in the pig. Interestingly, in the sheep, the two retia are connected across the midline by a few bridging vessels, whereas the connection between the retia in the pig is much more extensive and appears to be a single structure.

The relationship between the pattern and volume of anatomic retia anastomosis and the functions of physiologic flow autoregulation is yet to be investigated. Because of the differences in the anatomic rete structure between the sheep and the pig, the sheep actually has a double AVM nidus as compared with the single nidus in the pig. This difference may offer an opportunity to investigate the situation in which multiple AVMs are involved.

The techniques used to create the AVM model in sheep are rather simple. The crucial part of the method is to create an anastomosis surgically between the CCA and EJV, which are quite superficial in sheep. The technique can be performed by nonsurgically trained research personnel. Most important, there is no need to embolize carotid artery branches in order to develop the in vivo functional AVM model. Endovascular occlusion requires sophisticated endovascular techniques and special skills familiar only to neurointerventionists. This model also facilitates the rapid production of a large number of animal models for training courses. Cost-effectiveness is another important factor of this AVM model. Elimination of the need to occlude several carotid artery branches with expensive materials, such as microcatheters, microwires, and detachable balloons, decreases the cost. The costs for training and research will be consequently reduced.

Conclusion

This study demonstrated the feasibility of creating a cerebral AVM model in sheep with a simple technique. The model is attractive because: 1) it provides arterial feeders, a nidus with high flow, and a draining vein, which are considered the morphologic and hemodynamic features of cerebral AVMs; 2) the technique used to create this model is simple, cost-effective, and does not require sophisticated neurointerventional skills; 3) it eliminates the need for endovascular occlusion of multiple carotid artery branches; 4) the use of this model reduces the cost of creating an animal model for research or training purposes; and 5) it is possible to create a large number of models for hands-on training courses over a short period of time.

Acknowledgment

We are indebted to Rafael Lima-Rodriquez, DVM for his excellent assistance in anesthesia and to Anders Lunderquist, MD for his critical review of this study.

References

1. Drake CC. **Cerebral arteriovenous malformation: considerations for and experience with surgical treatment in 166 cases.** *Clin Neurosurg* 1979;26:145–208
2. Luessenhop AJ, Rosa A. **Cerebral arteriovenous malformation: indications for and results of surgery, and the role of intravascular techniques.** *J Neurosurg* 1984;60:14–22
3. Crawford PM, West CR, Chadwick DW, Shaw MDM. **Arteriovenous malformation of the brain: natural history in unoperated patients.** *J Neurosurg Psychiatry* 1986;49:1–10
4. Graf CJ, Perret GE, Torner JC. **Bleeding from cerebral arteriovenous malformations as part of their natural history.** *J Neurosurg* 1983;58:331–337
5. Massoud TF, Ji C, Viñuela F, et al. **An experimental arteriovenous malformation model in swine: anatomic basis and construction technique.** *AJNR Am J Neuroradiol* 1994;15:1537–1545
6. Moore BJ, Holmes KR, Xu LX. **Vascular anatomy of the pig kidney glomerulus: a qualitative study of corrosion casts.** *Scanning Microsc* 1992;6:887–898
7. Lee DL, Wriedt CH, Pelz DM, Fox AJ, Viñuela F. **Evaluation of three embolic agents in pig rete.** *AJNR Am J Neuroradiol* 1988;10:773–776
8. Lylyk P, Viñuela F, Vinters HV, et al. **Use of a new mixture for embolization of intracranial vascular malformations: preliminary experimental experience.** *Neuroradiology* 1990;32:304–310
9. De Salles AAF, Solberg TD, Mischel P, Massoud TF, Plasencia A, Goetsch S. **Arteriovenous malformation animal model for radiosurgery: the rete mirabile.** *AJNR Am J Neuroradiol* 1996;17:1451–1458
10. Daniel PM, Dawes DK, Prichard MML. **Study of the carotid rete and its associated arteries.** *Philos Trans R Soc Lond B Biol Sci* 1953;237:173–208
11. Backer MA, Hayward JN. **The influence of the nasal mucosa and the carotid rete upon hypothalamic temperature in sheep.** *J Physiol (London)* 1968;198:561–579
12. Bernstein MH, Duran HL, Pinshow B. **Extrapulmonary exchange enhances brain oxygen in pigeons.** *Science* 1984;226:564–566
13. McFarland WL, Jacobs MS, Morgane PJ. **Blood supply to the brain of the dolphin, Tursiops truncatus, with comparative observations on special aspects of the cerebrovascular supply of other vertebrates.** *Neurosci Biobehav Rev* 1979;3(Suppl 1):1–93
14. Isoda K, Fukuda H, Takamura N, et al. **Arteriovenous malformation of the brain: histological study and micrometric measurement of abnormal vessels.** *Acta Pathol Jpn* 1981;31:883–893
15. Brothers MF, Kaufmann JCE, Fox AJ, Deveikis JP. ***n*-Butyl 2-cyanoacrylate–substitute for IBCA in interventional neuroradiology: histopathologic and polymerization time studies.** *AJNR Am J Neuroradiol* 1989;10:777–786
16. Massoud TF, Ji C, Viñuela F, et al. **Laboratory simulations and training in endovascular embolotherapy with a swine arteriovenous malformation model.** *AJNR Am J Neuroradiol* 1996;17:271–279